in the separated region. The frequency of these movements was a maximum near the separation and reattachment points.

Figure 4 shows a typical correlogram in the separated region. This oscillatory nature in the separation bubble is due to the pronounced periodicity shown in Fig. 2.

The length of the separated region as determined by the different measurement techniques varies considerably. The pitot-pressure surveys and surface skin-friction data indicated the shortest region (186–190 cm). Both the surface pressure data (between infection points) and oil flow results indicated a slightly larger region (approximately 184–191 cm). Finally the power spectra and correlation measurements indicated a separated region even greater in extent (approximately 183–194 cm). These results suggest a model for turbulent boundary-layer separation similar to previous incompressible measurements[4]; that is, the onset and reattachment locations of separation are intermittent and only where the flow is reversed at least 50% of the time will the time averaged pitot-pressure and skin-friction measurements indicate separated flow while the instantaneous thin-film measurements are sensitive to regions which are separated for only a small fraction of time.

References

[1] Owen, F. K. and Horstman, C. C., "On the Structure of Hypersonic Turbulent Boundary Layers," *Journal of Fluid Mechanics*, Vol. 53, June 1972, pp. 611–636.

[2] Owen, F. K., "Transition Experiments on a Flat Plate at Subsonic and Supersonic Speeds," *AIAA Journal*, Vol. 8, No. 3, March 1970, pp. 518–523.

[3] Owen, F. K. and Horstman, C. C., "Hypersonic Transitional Boundary Layers," *AIAA Journal*, Vol. 10, No. 6, June 1972, pp. 769–775.

[4] Sandborn, V. A. and Liu, C. Y., "On Turbulent Boundary-Layer Separation," *Journal of Fluid Mechanics*, Vol. 32, May 1968, pp. 293–304.

Stability of Flow through Porous Plates: Coalescent Jets Effect

Marcos Pimenta* and Robert J. Moffat†
Stanford University, Stanford, Calif.

Introduction

THE main purpose of our experiments has been the study of turbulent boundary-layer development over smooth or rough porous plates with transpiration. Special treatment is given to heat-transfer studies, partly motivated by the current interest in protecting surfaces from hot streams in combustion chambers, turbines, and other applications.

During the qualification runs of the recently completed HMT apparatus for roughness studies, tests were conducted to determine the uniformity in porosity of the plates. These tests showed anomalous results: the flow through the plates seemed to coalesce into definite jets rather than come through the plate in a uniform manner. It was feared that this jetting action could appear even in the presence of a shear flow and have some effect on our boundary-layer heat-transfer measurements. This, in fact, motivated a more detailed analysis.

As it has been pointed out earlier by several authors, the flow through porous screens can under certain conditions present instabilities. A similar result has been observed for flow through permeable plates. In our present experiment, two different plates were investigated, both constituted of small spheres stacked in the densest arrangement and sintered together. One with 0.005-in.-diam spheres and the other, 0.050-in.-diam spheres. The main feature of the flow is the formation of jets leaving the surface which coalesce with each other in a spatially random but repeatable manner. This phenomenon occurs once the air leaving the porous surface exceeds a certain critical velocity. A quasi-hysteresis effect has also been observed. Once the jets have coalesced, their pattern is preserved even at air surface velocities smaller than the critical velocity. The plate made of the smaller particles has a larger critical velocity and a much finer jet pattern. Finally, it has been determined that the heat transfer from the plates to a free-stream flowing over them is not enhanced when the transpiration surface velocity exceeds the critical velocity. This observation suggests that the shear flow over the plates may stabilize the jets, preserving a uniform transpiration to a much higher value of velocity.

Received March 15, 1974; revision received June 3, 1974.

Index categories: Boundary Layers and Convective Heat Transfer—Turbulent; Jets, Wakes, and Viscid-Inviscid Flow Interactions.

* Graduate Student, Department of Mechanical Engineering.

† Professor, Department of Mechanical Engineering.

Previous Works

Most existing reports of flow instabilities behind porous surfaces refer to two-dimensional flows behind screens and rod grids. By flow instability, we mean here the coalescence of jets behind the porous surface. The first experimental work was presented by MacPhail.[1] In his case he was interested in solving the problem of obtaining a uniform velocity distribution in a duct downstream of a 90° bend followed by a sudden expansion.

An experimental investigation carried out by von Bohl[3] studied the stability behind a grid of rods in a closed duct. His main conclusion was that, depending on the open area ratio of the grid, he was able to get stable and unstable flows. The study by von Bohl showed that open ratios of 0.63 and 0.54 corresponded to stable and unstable conditions, respectively.

Corrsin[4] also reports a study on the stability of two-dimensional flow through a grid of rods with an open area ratio of 0.17. He observed unstable flow so irregular that sufficiently far from the grid one could not see any evidence of the flow coming from a regular row of jets. His main interest was also, primarily, in a way of controlling it and overcoming the instability.

Finally, Bradshaw,[5] in a more recent paper, describes the nonuniformity problem that he obtained in a spanwise shear stress distribution in a two-dimensional wind tunnel. As he states, the last wire mesh screen of the tunnel screen arrangement was responsible for the nonuniformity. He concluded that a 0.57 open ratio is the minimum value to avoid instability. He also suggests a minimum distance between screens.

Morgan[2] and Bradshaw[5] attribute the cause of the instabilities to the coagulation of the jets coming out from the screens, which in its turn depends upon the entrainment of air by individual jets from the wakes between them. A critical open area ratio does exist, below which the entrainment is so large that different jets coalesce together.

Besides these references, very few authors report studies for the three-dimensional case. Morgan[2] refers to perforated plates for which he says there is no critical open area ratio. For the same case as Bradshaw, i.e., wire screen, he mentions a critical ratio of 0.5.

Schubauer[6] mentions that the coalescence of jets in certain circumstances for open area ratios of less than 0.5 can cause spatial variations in velocity as well as a higher turbulence level.

Present Investigation

Our present investigation was done using two of the Stanford HMT group wind tunnels. Both have been designed for turbulent boundary-layer studies with transpiration (for description of apparatus, see Ref. 7). The one reserved to smooth plate studies has 24 porous plates made from 0.005-in.-diam particles, the other, for roughness-effect studies, has 24 porous plates made from 0.050-in.-diam spheres sintered together.

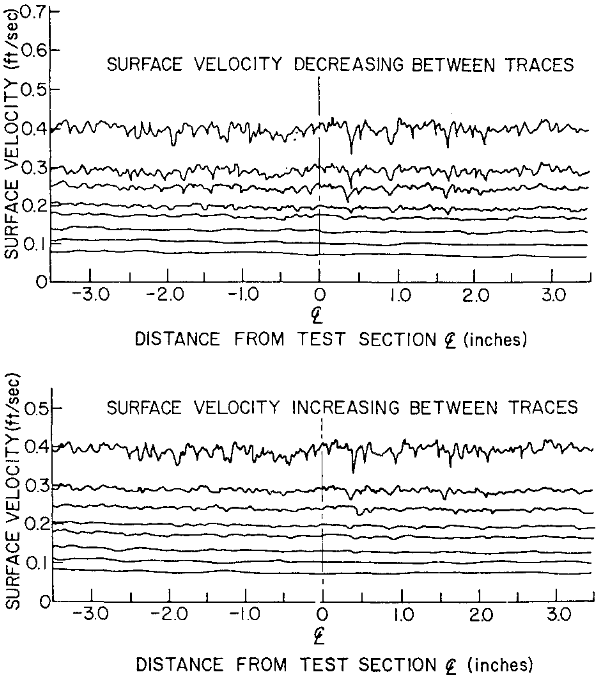

Fig. 1 Velocity distribution above roughness rig section.

This study resulted from the roughness rig qualification tests, in particular, from an attempt to map the plate permeability. A calibrated constant current-type hot-wire anemometer was supported on a traversing mechanism on the test section side walls. The traverses were made at a height of about $\frac{1}{8}$ in. above the plate surface. The output from the anemometer was run directly into an x-y plotter and a resistance built into the traversing mechanism drove the plotter such that pen movement across the graph corresponded approximately to probe movement over the plates. The graphs thus obtained corresponded to a map of the surface velocity of air delivered through the plates. A typical graph is shown in Fig. 1 for different air velocities. The surface velocity traces appear very lumpy, and the formation of jets becomes evident at high blowing rates, being clearly a function of space, but not of time. The nonuniformity in velocity is several percent, and the spanwise period of the velocity disturbances appears to be several sphere diameters. The spikiness in a separate test has proved to persist all the way to the wall and to have normal attenuation away from it.

The tests were performed over a wide range of surface velocities. Referring to Fig. 1, surface velocity traverses have been traced and superimposed on a single graph. The top graph shows the results obtained starting at a high surface velocity and reducing it. The magnitude of the nonuniformity is reduced as the surface velocity is reduced, but it is still clearly present at 0.21 fps. The velocity trace is much smoother at 0.17 fps, and is almost completely smooth for lower surface velocities. This indicates a critical surface velocity at or near 0.18 fps. The lower graph shows results obtained starting at low surface velocities and increasing. Here the traces remain smooth for velocities up to 0.24 fps, suggesting that there is something akin to hysteresis associated with this process. As the surface velocity is decreased from a high value, the jet coalescence persists to much lower surface velocities than first caused coalescence, when the surface velocity was increased. If we superimpose the surface velocity traverses for the highest blowing rate, we can observe a remarkable similarity, specifically if we consider the position of the peaks in velocity. This confirms the phenomenon we are observing. The jets formation is spatially determinate and not time-dependent, given the reproducibility of the peaks in velocity.

The critical velocity so far referred to must then be a porous plate characteristic. A second set of similar experiments was conducted in the other wind tunnel. Figure 2 shows a characteristic graph obtained for the 0.005-in.-diam particle porous plates. Again the flow shows the same lumpy appearance above a critical surface velocity that seems to be higher than the previous one. Here the structure of the velocity traces appeared much finer grained than that observed over the rough surface.

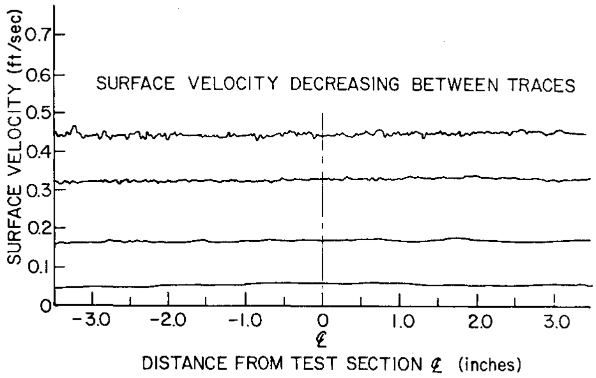

Fig. 2 Velocity distribution above smooth porous surface.

After the presence of the jetting action was confirmed, we investigated the possible effect on boundary-layer heat-transfer measurements over those plates. The jetting effect had not been observed in the smooth plate wind tunnel. This was attributed to the fact that never, under operating conditions, did the surface velocity become larger than the critical velocity (as determined by our experiments). Returning to the rough plate apparatus, a complete set of heat-transfer runs was then made with several different blowing rates. In this case the operating modes would have surface velocities larger than this critical one. In both cases the heat-transfer measurements were averaged over an area very large compared to the jets' size.

Figure 3 shows the ratio of the blown to the unblown Stanton number at the same x-Reynolds number plotted against $\ln(1+B)/B$, where $B = St/F$ is the blowing parameter and $F = \rho_o v_o / \rho_\infty U_\infty$ the so-called blowing fraction. Note that subscripts o and ∞ refer to wall and freestream values, respectively. Moffat[7] has shown that this form of plot correlates the blown and unblown data. In our case the critical surface velocity corresponds to a blowing fraction $F \simeq 0.0022$. No observable discontinuity is seen when F is doubled from 0.002 to 0.004. This is considered an indication that the jetting effect is not present, or at least has no influence on the heat-transfer measurements. If the jetting effect had affected the value of Stanton number, then St/St_o would have shown a jump at the value of blowing for which the jetting became important.

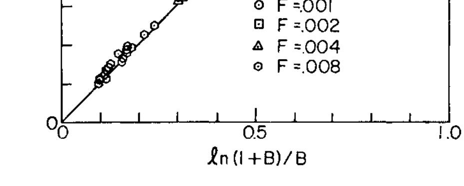

Fig. 3 Stanton number ratio (St/St_o) vs $\ln(1+B)/B$.

Conclusion

The appearance of instabilities resultant from coalescence of neighboring jets has been observed and confirmed for flow through porous plates. This flow instability appears similar to those previously reported by Morgan[2] and Bradshaw.[5] A critical velocity exists, above which instabilities appear. This critical velocity depends on the plate porosity. The presence of a shear flow over the plate seems to stabilize the jets. No effect was observed in heat-transfer measurements with transpiration.

References

[1] MacPhail, D., ARC R & M 1876, 1939, Aeronautical Research Council, London, England.

[2] Morgan, P. G., "The Stability of Flow Through Porous Screens," *Journal of the Royal Aeronautical Society*, Vol. 64, 1960, pp. 359–362.

[3] von Bohl, D., *Ingenieur Archiv*, Vol. 11, No. 4, 1940, p. 295.

[4] Corrsin, S., ACR 2H24, 1944, NACA.

[5] Bradshaw, P., "The Effect of Wind-Tunnel Screens on Nominally Two-Dimensional Boundary Layers," *Journal of Fluid Mechanics*, Vol. 22, Pt. 3, 1965, pp. 679–687.

[6] Schubauer, G. M., *Journal of the Aeronautical Sciences*, Vol. 14, 1947, p. 4.

[7] Moffat, R. J. and Kays, W. M., "The Turbulent Boundary Layer and Porous Plate: Experimental Heat Transfer with Uniform Blowing and Suction," Rept. HMT-1, 1967, Thermosciences Div., Dept. of Mechanical Engineering, Stanford University, Stanford, Calif.

Flowfield in the Combustion Chamber of a Solid Propellant Rocket Motor

R. DUNLAP,* P. G. WILLOUGHBY,† AND R. W. HERMSEN‡
United Technology Center, Sunnyvale, Calif.

Introduction

AN accurate description of the three-dimensional flowfield in a rocket chamber is required in order to develop further understanding and more precise prediction techniques in areas such as metal combustion, metal oxide particle growth, erosive propellant burning, and damping of acoustic waves. In connection with the acoustic damping problem, Culick[1] presented an analytical solution for the steady, inviscid, incompressible flow in an internal-burning cylindrical grain configuration wherein the fluid was assumed to enter normal to the burning surface. This flow has the interesting feature that while satisfying the inviscid equations of motion it also satisfies the no-slip boundary condition of a viscous fluid. In this Note it is shown that this same velocity field also closely satisfies the viscous equations of motion, except in a small region near the head-end of the chamber. The expectation that the Culick solution may therefore accurately represent the real flow was verified by an experiment carried out in a porous tube apparatus.

Applicability of Inviscid No-Slip Solution to Actual Flow

The solution derived by Culick,[1] for the motion of an incompressible and inviscid fluid entering at a uniform rate normal to the wall of a circular cylinder which is closed at $z = 0$, may be written

$$u(r, z) = v_w \pi (z/r_w) \cos(\pi r^2/2r_w^2) \tag{1}$$

$$v(r, z) = (-v_w r_w/r) \sin(\pi r^2/2r_w^2) \tag{2}$$

$$P(r, z) = P(o, o) - (\rho/2)[v^2(r, z) + u^2(o, z)] \tag{3}$$

Received March 29, 1974.

Index categories: Nozzle and Channel Flow; Viscous Nonboundary-Layer Flows; Solid and Hybrid Rocket Engines.

* Senior Staff Scientist. Member AIAA.

† Senior Scientist.

‡ Manager, Physical Sciences Laboratory. Associate Fellow AIAA.

where P is the pressure, u and v are the velocity components in the z and r directions, respectively, and v_w is the magnitude of the wall velocity. Since this flow satisfies the viscous no-slip condition along the boundary $r = r_w$, the question arose as to what degree it may represent the entire viscous flowfield. To be an accurate solution to the viscous equations of motion, the flow represented by Eqs. (1–3) must also satisfy the condition that the net viscous force acting on a fluid element is small compared to the net pressure force. That is, in this event the flow satisfies both the inviscid and viscous equations of motion while also satisfying the no-slip boundary condition.

The ratio of magnitudes of the differential viscous force on a fluid element to the differential pressure force for this flowfield may be written

$$FR = \frac{|\text{net viscous force}|}{|\text{net pressure force}|} = \mu \left\{ \frac{\left[\frac{\partial^2 u}{\partial r^2} + \frac{\partial^2 u}{\partial z^2} + \frac{1}{r}\frac{\partial u}{\partial r}\right]^2 + \left[\frac{\partial^2 v}{\partial z^2} + \frac{\partial^2 v}{\partial r^2} + \frac{\partial}{\partial r}\left(\frac{v}{r}\right)\right]^2}{\left(\frac{\partial P}{\partial z}\right)^2 + \left(\frac{\partial P}{\partial r}\right)^2} \right\}^{1/2} =$$

$$\frac{4}{Re} \left\{ \frac{\left[\sin\left(\frac{\pi r^2}{2r_w^2}\right) + \frac{\pi r^2}{2r_w^2}\cos\left(\frac{\pi r^2}{2r_w^2}\right)\right]^2 + \frac{r^2}{4z^2}\sin^2\left(\frac{\pi r^2}{2r_w^2}\right)}{1 + \frac{r_w^8 \sin^2 \pi r^2/2r_w^2}{\pi^4 z^2 r^6}\left[\frac{r^2\pi}{r_w^2}\cos\left(\frac{\pi r^2}{2r_w^2}\right) - \sin\left(\frac{\pi r^2}{2r_w^2}\right)\right]^2} \right\}^{1/2}$$

where $Re = 2\rho v_w r_w/\mu$ is the Reynolds number. This ratio satisfies the inequality

$$FR < \frac{5.56}{Re}\left(1 + \frac{r^2}{7.72z^2}\right)^{1/2}$$

Thus, when the Reynolds number is large the viscous stresses are indeed negligible compared to pressure forces except in the narrow region $z/r = 0(1/Re)$ at the head end of the chamber.

In concluding that Eqs. (1–3) closely represent the actual flow in a rocket chamber, where Re is the order of 10^4 to 10^5, it should be emphasized that the abovementioned arguments are based on the assumption of laminar flow. However, the same conclusion would be reached for turbulent flow with this velocity distribution as long as the net force due to Reynolds stress acting on a fluid element is small compared to the net pressure force.

Experiment to Determine Chamber Flowfield

To test the above reasoning, as well as possible implications of turbulence, a cold flow experiment was devised in which a series of five cylindrical porous tubes were used to simulate the propellant surface (see Fig. 1). The porous tubes were sintered bronze having a wall thickness of 0.10 in. and a pore size in the range 5–15 μ. Ambient temperature nitrogen entered the chamber uniformly through the porous tubes and exited to the atmosphere through an aluminum section which joined smoothly to the last porous tube. Centerline velocity distributions were measured with a hot-wire anemometer made from 0.00035-in. by 0.10-in.

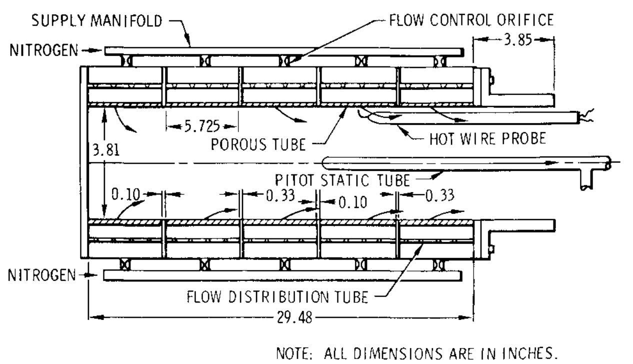

Fig. 1 Experimental apparatus for cold flow simulation of rocket chamber flowfield.